Propulsion and Power Research 2015;4(2):84–90

HOSTED BY
ELSEVIER

http://ppr.buaa.edu.cn/

Propulsion and Power Research

www.sciencedirect.com

ORGINAL ARTICLE

Comparison between the volumetric flow rate and pressure distribution for different kinds of sliding thrust bearing

O. Pourmehran[a], M. Rahimi-Gorji[a,*], M. Gorji-Bandpy[a], M. Baou[b]

[a]*Faculty of Mechanical Engineering, Babol Noshirvani University of Technology, Babol, Iran*
[b]*Faculty of Mechanical Engineering, Shahrood University of Technology, Shahrood, Iran*

Received 17 October 2014; accepted 21 January 2015

KEYWORDS

Non-parallel plate bearing;
Hydrodynamic sliding bearing;
Incompressible lubricant flow;
Volumetric flow rate;
Exponential geometry

Abstract In this paper a hydrodynamic journal sliding bearing, forming with two nonparallel surfaces that the lower surface moves with a unidirectional velocity and the upper surface is stationary shaped with exponential geometry is verified mathematically. The values of volumetric flow rate and distribution of pressure for incompressible lubricant flow between two supports in several conditions of velocity with different variables are determined. The results indicate that by increasing the amount of constant (m), the maximum oil pressure in the bearing will face an extreme decrease, and also by increasing the α coefficient, the rate of volumetric flow rate will decrease.

1. Introduction

Bearings allow smooth and low friction motion between two surfaces loaded against each other. The motion can be either rotary (such as a shaft turning within housing) or linear (one machine element moving back and forth across another). The most basic bearing is the plain type that has no moving parts and it supports loads through sliding motion. Conversely, rolling-element bearings are subjected to very little sliding and the load is supported by numerous rolling members inside the bearing. In either situation, proper lubrication is essential to long bearing life. Plain bearings generally cost less than similarly sized rolling-element bearings, but rolling-element bearings generally can tolerate heavier loads and higher speeds. Bearings that support loads perpendicular to their axis of rotation are

*Corresponding author. Tel.: +9811332 240 48.
E-mail addresses: m69.rahimi@yahoo.com (M. Rahimi-Gorji), gorji@nit.ac.ir (M. Gorji-Bandpy).

Peer review under responsibility of National Laboratory for Aeronautics and Astronautics, China.

http://dx.doi.org/10.1016/j.jppr.2015.05.002

Nomenclature

u	x velocity (unit: m/s)
v	y velocity (unit: m/s)
w	z velocity (unit: m/s)
b	width of bearing (unit: m)
D	shaft diameter of rolling bearing (unit: m)
L	length of bearing (unit: m)
U	circumferential velocity (unit: m/s)
Q	volumetric flow (unit: m^3/s)
P	film pressure (unit: N/m^2)
h_1	minimum gap between the surfaces (unit: m)
F	external load (unit: N)
h	gap between the surfaces (unit: m)
P_{atm}	atmospheric pressure (unit: Pa)

Greek letters

ρ	fluid density (unit: kg/m^3)
α,β,m	constant

called radial-type whereas bearings supporting loads parallel to their axis of rotation are termed thrust bearings. Thrust bearing, used to support thrust load in rotating machinery consist of multiple pads, either fixed or pivoted. Research on oil flow through a lubricating groove carried out by Ettles [1] showed that about 85% of hot oil leaving the gap enters the next oil gap in the case of laminar flow. Later in his subsequent papers [2,3], Ettles proposed an idea of the “hot oil carry-over factor”. Values for this factor were assessed on an experimental basis as a function of the sliding speed and size of the gap between the bearing pads. Some principles of lubrication are presented in [4].

Other models of oil flow in the bearing groove were proposed by Vohr [5], who presented a model including a variety of heat exchange phenomena in the groove, and Heshmat and Pinkus [6] and Kicinski [7], who calculated both the flow of oil and heat balance. Some phenomena in the oil gap are described with increasing accuracy by these derived models. Various arrangements aimed at improving the scoring of hot oil layer moving with the runner have been proposed [8–16]. In this paper volumetric flow rate and distribution of pressure are presented for several conditions. The sliding bearing is presently widely used by industry in the form of thrust bearing [17]. Hydrodynamic thrust bearings are used mainly in large and heavy equipment such as: ships propeller shafts (tail shafts), fans and pumps, large steam and gas turbines engines [14], vertical axis machines such as coal crushers [15] and finally heat exchanger [16,18].

2. Hydrodynamic theory of lubrication

The hydrodynamic theory of lubrication of journal bearings is older than a century. In his famous experiment, Tower has shown the pressure distribution in the lubricating oil film in the clearance of journal bearings [15,19]. Also in this year Petroff measured the friction torque of oil lubricated sliding bearings and created a formula to calculate it. Knowing the results of experiments made by Tower and Petroff, Reynolds evolved the basic equation of hydrodynamic theory of lubrication of journal bearings from the Navier-Stokes equations using many assumptions. The Reynolds equation cannot be solved in full form therefore it is necessary to make some simplifications to get a simple solution. There are two general simplifications: the infinitely long bearing ($b/d=\infty$, b: width of the bearing and d: shaft diameter of rolling bearing) and the short bearing assumption ($\partial p/\partial z \gg \partial p/\partial z$) [1]. In 1902 Sommerfeld solved the Reynolds equation making special boundary conditions for pressure distribution in tangential direction which according to him is called Sommerfeld conditions resulting in a central symmetric solution. In the practice the often used boundary conditions are the following: the Sommerfeld conditions $p_{\varphi=\pi}=0$ and the Reynolds conditions $\left(\frac{\partial^2 p}{\partial \varphi^2}\right)_{\varphi=\pi}=0$ [15]. Using these assumptions many solutions were achieved during the last century for static and also dynamic operating conditions. Nowadays, numerical methods are often used for solving the Reynolds equation and can be seen in Kozma [20–28].

3. Description of the optimization problem

The sliding bearings consist of at least two contact surfaces. One of the surfaces is moving with a relative velocity U as it can be seen in Figure 1 gap between the sliding surfaces is filled with incompressible lubricant. Concerning the friction state in the sliding bearing, three cases are possible:

3.1. Dry friction

Where the surfaces are in full contact. Failure danger of the sliding surfaces is large, because of the roughness of the

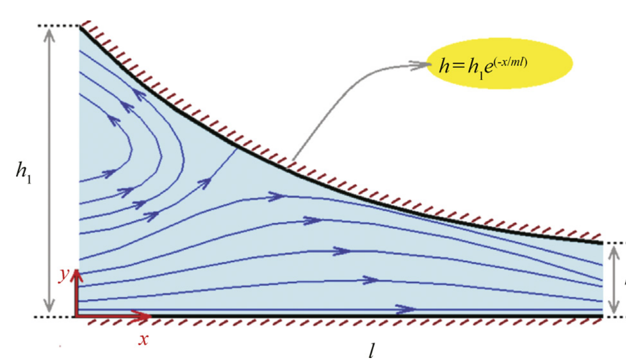

Figure 1 Geometry of physical model.

surfaces. During the operation and maintenance of the bearing this case should be avoided if possible.

3.2. Mixed friction

States between the fluid friction and dry friction. This is possible during the running - in period or in the starting and stopping process, because the velocity is not enough to maintain the necessary lubricant flow in the gap.

3.3. Fluid friction

In this case the surfaces are not in contact, the pressure in the lubrication film is in equilibrium with the external load F. The sliding bearings are supposed to operate in these conditions; therefore this is the most important case for the user and for the designer [29].

In this paper two nonparallel surfaces that the lower surface moves with a unidirectional velocity U as shown in Figure 1 and the upper surface is stationary and supposed with Exponential geometry as shown in Eq. (2) are considered.

The gap between the sliding surfaces is filled with incompressible lubricant. About geometry of sliding as shown in Eq. (1) this sets named hydrodynamic journal sliding bearing. The sliding direction is such that a convergent fluid film is formed between the surfaces to produce hydrodynamic pressure.

It is assumed that the width of the bearing, b, is much greater than its length, l, therefore most of the flow through the gap between the two surfaces occurs in the direction of the x axis. The governing equations are as follow:

$$h = h_1 e^{\left(\frac{-x}{ml}\right)} \tag{1}$$

$$U = \beta x^{a} \tag{2}$$

where $h_1 = h_{min}$ is the minimum gap between the surfaces and α, β are variable parameters that we produced for commercial bearing as special data to compare in useful curve to understanding optimum value.

From the Navier-Stokes equation we have [30]

$$\rho\left(\frac{\partial u}{\partial t} + u\frac{\partial u}{\partial x} + v\frac{\partial u}{\partial y}\right) + \frac{\partial p}{\partial x} = \mu\left(\frac{\partial^2 u}{\partial x^2} + \frac{\partial^2 u}{\partial y^2}\right) \tag{3}$$

And the boundary conditions are:

$$@y = 0 \rightarrow u = U$$

$$@y = h \rightarrow u = 0 \tag{4}$$

Solving this equation in a special condition we obtain [30]

$$u = \frac{1}{2\mu}\frac{\partial P}{\partial x}(y^2 - yh) + U\left(1 - \frac{y}{h}\right) \tag{5}$$

$$Q = \int_0^h u\,dy \rightarrow Q = \frac{3}{4} U h_1 \frac{e^{\frac{2}{m}} - 1}{e^{\frac{3}{m}} - 1} \tag{6}$$

In case of fluid friction the pressure distribution in the lubricant film can be determined from Eqs. (5) and (6). According to the above equations, the pressure distribution depends on the gap form function $h(x,z)$, the viscosity of the lubricant μ, the relative velocity U and the parameter of m.

$$P = P_{atm} + \frac{3\mu U l m}{h_1{}^2}\left[\left(e^{\frac{2x}{ml}} - 1\right) - \frac{e^{\frac{2}{m}} - 1}{e^{\frac{3}{m}} - 1}\left(e^{\frac{3x}{ml}} - 1\right)\right] \tag{7}$$

Table 1 Physical parameters.

μ/(Pa · s)	h_1/m	ρ/(kg/m^3)	L/cm	U/(m/s)
0.1	0.0001	889	5	1

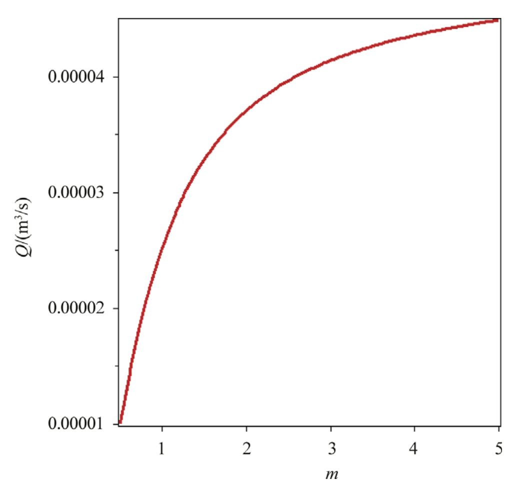

Figure 2 Volumetric flow rate vs. m when U=1 m/s.

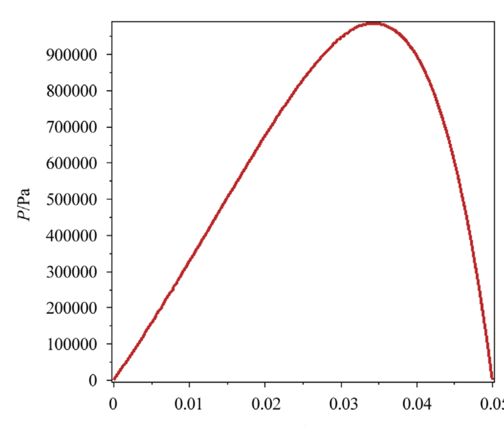

Figure 3 Pressure distribution against position, U=1 m/s and m=0.5.

For drawing these equations we must introduce physical parameters then with refer to industries fluid lubricant, ordinary oil is supposed, therefore as shown Table 1.

For more consideration, one must care to these following diagrams (Figure 2 and Figure 3).

This part presents the differences between the profiles of relative velocities with reference to Eq. (2).

After solving the Navier-Stokes equations for this model for obtaining volumetric flow and film pressure, we have the following equations whereas the properties are shown in the Figures 4–7.

$$Q = \frac{1}{12\mu} \times \left\{ \frac{18\mu\beta h_1 \int_0^l x^\alpha e^{\frac{2x}{ml}}dx - \frac{3\rho\beta^2}{2} l^{2\alpha} {h_1}^3}{ml(e^{\frac{3}{m}}-1)} \right\} \tag{8}$$

$$P = P_{atm} + \frac{6\mu\beta}{{h_1}^2}\left(ml^2 e^{\frac{2}{m}} - \frac{m^2 l^2}{4} e^{\frac{2}{m}} + \frac{m^2 l^2}{4}\right) \times \left(1 - 3\frac{e^{\frac{3x}{ml}}-1}{e^{\frac{3}{m}}-1}\right) + 1.5\rho\beta^2 l^2 \frac{e^{\frac{3x}{ml}}-1}{e^{\frac{3}{m}}-1} - 0.5\rho\beta^2 x^2 \tag{9}$$

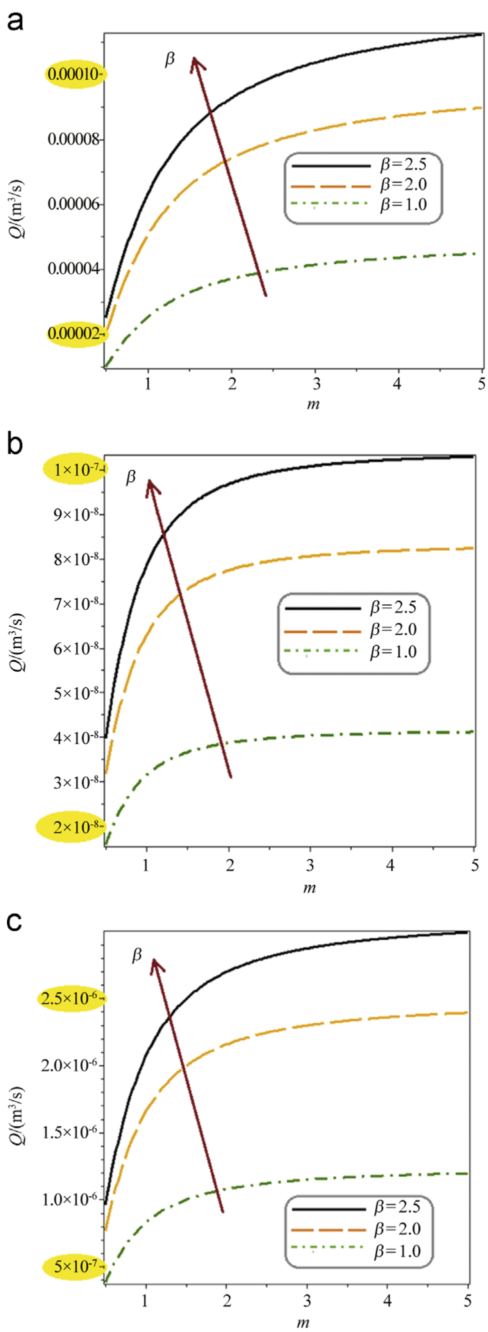

Figure 4 Volumetric flow rate against m when (a) $\alpha = 0, \beta = 1, 2, 2.5$, (b) $\alpha = 1, \beta = 1, 2, 2.5$, and (c) $\alpha = 2, \beta = 1, 2, 2.5$.

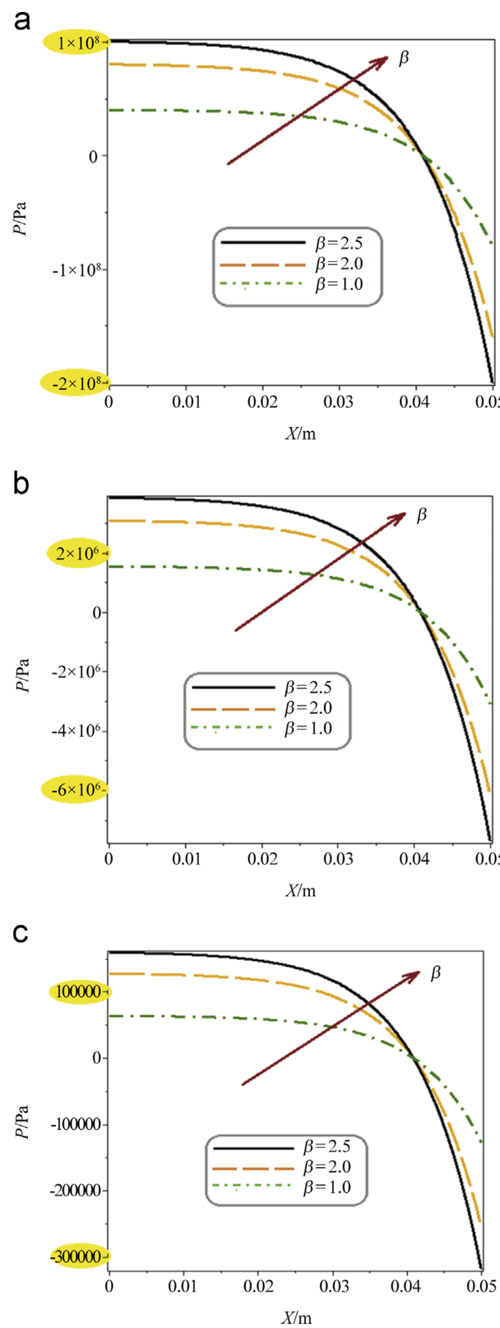

Figure 5 Pressure disturbance vs. x when (a) $\alpha = 0, m = 0.5, \beta = 1, 2, 2.5$, (b) $\alpha = 1, m = 0.5, \beta = 1, 2, 2.5$, and (c) $\alpha = 2, m = 0.5, \beta = 1, 2, 2.5$.

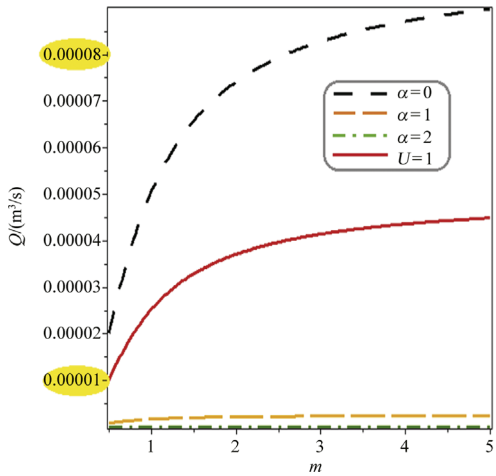

Figure 6 Volumetric flow rate against m when $\beta=2$.

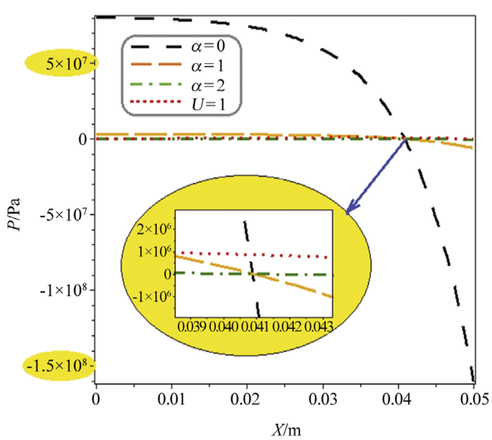

Figure 7 Pressure disturbances vs. x when $\beta=2$.

In the following steps these equations are solved and the results are presented by different curves with different pressure and the parameters of α, m and β as follows;

$\alpha=0,1,2$

$m=0.5,1,5$

$\beta=1,2,2.5$

Step 1:
For $\alpha=0$ the following equations is obtained;

$$Q=0.25\times\frac{3\beta h_1(e^{\frac{2}{m}}-1)-\frac{\rho\beta^2}{2\mu ml}{h_1}^3}{e^{\frac{3}{m}}-1} \tag{10}$$

$$P=P_{atm}+\frac{3\mu\beta ml}{{h_1}^2}\left\{(e^{\frac{2}{m}}-1)\times\left(1-3\frac{e^{\frac{3x}{ml}}-1}{e^{\frac{3}{m}}-1}\right)\right\} -\frac{\rho\beta^2}{2}\left(1-3\frac{e^{\frac{3x}{ml}}-1}{e^{\frac{3}{m}}-1}\right) \tag{11}$$

Step 2:
For $\alpha=1$;

$$Q=\frac{\frac{3}{16}\beta h_1 ml\left(\frac{2}{m}e^{\frac{2}{m}}-e^{\frac{2}{m}}+1\right)-\frac{\rho\beta^2}{8\mu m}l{h_1}^3}{(e^{\frac{3}{m}}-1)} \tag{12}$$

$$P=P_{atm}+\frac{6\mu\beta}{{h_1}^2}\left(ml^2e^{\frac{2}{m}}-\frac{m^2l^2}{4}e^{\frac{2}{m}}+\frac{m^2l^2}{4}\right) \times\left(1-3\frac{e^{\frac{3x}{ml}}-1}{e^{\frac{3}{m}}-1}\right)+1.5\rho\beta^2l^2\frac{e^{\frac{3x}{ml}}-1}{e^{\frac{3}{m}}-1}-0.5\rho\beta^2x^2 \tag{13}$$

Step 3:
For $\alpha=2$;

$$Q=\frac{1}{(e^{\frac{3}{m}}-1)}\left(1.5\beta h_1\left\{\frac{l^2}{2}e^{\frac{2}{m}}-\frac{ml^2}{2}e^{\frac{2}{m}} +\frac{m^2l^2}{4}e^{\frac{2}{m}}-\frac{m^2l^2}{4}\right\}\right) -\frac{\frac{\rho\beta^2l^2{h_1}^3}{8\mu m}}{(e^{\frac{3}{m}}-1)} \tag{14}$$

$$P=P_{atm}+\frac{6\mu\beta}{{h_1}^2}\left\{1-3\frac{e^{\frac{3x}{ml}}-1}{e^{\frac{3}{m}}-1}\right\} \times\left\{\frac{ml^3}{2}e^{\frac{2}{m}}-\frac{m^2l^3}{2}e^{\frac{2}{m}}+\frac{m^3l^3}{4}e^{\frac{2}{m}}-\frac{m^3l^3}{4}\right\} -\frac{\rho\beta^2x^4}{2}-1.5\rho\beta^2l^4\frac{e^{\frac{3x}{ml}}-1}{e^{\frac{3}{m}}-1} \tag{15}$$

4. Result and discussion

4.1. *Volumetric flow rate against m*

Figure 4 presents the rate of volumetric flow in three different bettacoefficient with change of m. It reveals the rate of Q is increase when the β increase and also with decreasing the α.

4.2. *Pressure disturbance vs. x*

Figure 5 presents the rate of pressure in three different β coefficient with change of x. It show, by increasing α, where the relative pressure is zero, it will occur in shorter lengths and with increase in β, alteration in pressure quantities will increase.

According to Figure 6 and Figure 7, understand that by increasing α coefficient, the rate of Q and P decrease.

5. Conclusions and recommendations

In this paper the values of volumetric flow rate and distribution of pressure for incompressible lubricant flow between two supports in several conditions of velocity with different variables are determined. The results of this study can be summarized as follows:

(1) By increasing the β coefficient, the rate of volumetric flow rate will increase.
(2) By increasing the α coefficient, the rate of volumetric flow rate will decrease.
(3) With attention to practical issues we know that the more m decreases, it is better considering its functioning, and it will have a higher capacity of yield endurance, but due to structure problems an optimum amount is satisfactory.
(4) The more m increases the amount of volumetric flow rate will also increase.
(5) In cases of high m quantities, the manners of changes in volumetric flow rate are independent of m.
(6) As m increases, the maximum oil pressure in the bearing will face an extreme decrease.
(7) When α is stable, interchange for alterations in β, with decrease in spatial m in which comes to zero, it will tend towards higher points.
(8) As the amount of m increases the maximum pressure distribution curve will tend towards shorter lengths.
(9) By increasing α, where the relative pressure is zero, it will occur in shorter lengths.
(10) With increase in β, alteration in pressure quantities will increase.
(11) In exchange for α equal to β alterations in the pressure distribution diagram, there will be no changes where relative pressure is zero and it will be stable.
(12) With decrease in β alterations in pressure distribution diagrams will curve towards higher m ratios.
(13) With increase in m, quantities and pressure changes will decrease.

References

[1] C.M. Ettles, Solutions for flow in a bearing groove, Proceedings of the Institution of Mechanical Engineers 182 (1967) 120–131.
[2] C.M. Ettles, Hot oil carry over in thrust bearings, Proceedings of the Institution of Mechanical Engineers 184 (12) (1969) 75–81.
[3] C.M. Ettles, Transient thermoelastic effects in fluid film bearings, Wear 79 (1) (1982) 53–71, URL ⟨http://www.sciencedirect.com/science/article/pii/0043164882902034⟩.
[4] Cameron, Principles of Lubrication, Longman, London, 1966.
[5] J.H. Vohr, Prediction of the operating temperature of thrust bearings, Journal of Tribology 103 (1), URL ⟨http://tribology.asmedigitalcollection.asme.org/article.aspx?articleid=1464625⟩.
[6] H. Heshmat, O. Pinkus, Mixing inlet temperatures in hydrodynamic bearings, Journal of Tribology 108 (2), URL ⟨http://tribology.asmedigitalcollection.asme.org/article.aspx?articleid=1458739&resultClick=3⟩.
[7] J. Kicin′ski, Models of heat exchange and flow in the bearing grooves and in the gaps between slider bearing pads, Transactions of the IFFM PAS, No. 347/1280/91, Gdan′sk, 1991.
[8] A.M. Mikula, R.S. Gregory, A comparison of tilting pad thrust bearing lubricant supply methods, Journal of Tribology 105 (1), URL ⟨http://tribology.asmedigitalcollection.asme.org/article.aspx?articleid=1465106⟩.
[9] F.J. Lin, S.Y. Chen, M.S. Huang, Adaptive complementary sliding-mode control for thrust active magnetic bearing system, Control Engineering Practice 19 (7) (2011) 711–722, URL ⟨http://www.sciencedirect.com/science/article/pii/S0967066111000463⟩.
[10] D. Guerin, L.F. Hall, An experimental comparison between three types of heavy duty thrust bearings, IME Proceedings of the Conference on Lubrication & Wear 79 (1957) 128–134.
[11] S. Glavatskikh, M. Fillon, R. Larsson, The significance of oil thermal properties on the performance of a tilting-pad thrust bearing, Journal of Tribology 124 (2), URL ⟨http://tribology.asmedigitalcollection.asme.org/issue.aspx?journalid=134&issueid=28705⟩.
[12] G. Rotta, Modeling of the oil film of a thrust bearing with the use of FEM, Proceedings of the sixth doctoral seminar, Gdan′sk 33 (2003) 55–62.
[13] Y. Li, G.Q. Xu, H.W. Deng, S.Q. Tian, Buoyancy effect on heat transfer in rotating smooth square U-duct at high rotation number, Propulsion and Power Research 3 (3) (2014) 107-120, URL ⟨http://www.sciencedirect.com/science/article/pii/S2212540X14000534⟩.
[14] G. Rotta, Modeling of the gap between thrust bearing pads, Tribology 35 (4) (2004) 196.
[15] M. Wasilczuk, G. Rotta, Modeling lubricant flow between thrust-bearing pads, Tribology International 41 (9-10) (2008) 908-913, URL ⟨http://www.sciencedirect.com/science/article/pii/S0301679X07001958⟩.
[16] M. Ghazikhani, M. Hatami, D.D. Ganji, M. Gorji-Bandpy, A. Behravan, G. Shahi, Exergy recovery from the exhaust cooling in a DI diesel engine for BSFC reduction purposes, Energy 65 (1) (2014) 44-51, URL ⟨http://www.sciencedirect.com/science/article/pii/S036054421301061X⟩.
[17] E. Baka, Calculation of the hydrodynamic load carrying capacity of porous journal bearing, Periodica Poly Technica Ser, Mech. Eng. 46 (1) (2002) 3–14, URL ⟨http://www.pp.bme.hu/me/article/view/1387⟩.
[18] M. Hatami, D.D. Ganji, M. Gorji-Bandpy, A review of different heat exchangers designs for increasing the diesel exhaust waste heat recovery, Renewable and Sustainable Energy Reviews 37 (2014) 168–181.
[19] S. Uno, M. Andoh, S. Namba, K. Mukai, Overview of recent tendencies in thrust bearings for hydrogenerators, Jap, J. Tribol 42 (2) (1997) 205–221, URL ⟨http://www.pp.bme.hu/me/article/view/1387/791⟩.
[20] S. Bhattrai, H. Tang, Comparative performance analysis of combined-cycle pulse detonation turbofan engines (PDTEs), Propulsion and Power Research 2 (3) (2013) 214–224, URL ⟨http://www.sciencedirect.com/science/article/pii/S2212540X13000229⟩.

[21] S.B. Glavatski, Laboratory research facility for testing hydrodynamic thrust bearings, in: Proceedings of the Institution of Mechanical Engineers, Part J: Journal of Engineering Tribology February 216 (1) (2002) 105–116, URL ⟨http://pij.sagepub.com/content/216/2/105.full.pdf⟩.

[22] Kozma, Load carrying capacity of dynamically loaded journal bearing, Periodical Polytechnic 40 (1995) 39-44.

[23] M. Rahimi-Gorji, O. Pourmehran, M. Hatami, D.D. Ganji, Statistical optimization of microchannel heat sink (MCHS) geometry cooled by different nanofluids using RSM analysis, European Physical Journal Plus 130 (2) (2015) 1–21 ⟨http://link.springer.com/article/10.1140/epjp/i2015-15022-8#page-1⟩.

[24] O. Pourmehran, M. Rahimi-Gorji, M. Hatami, S.A.R. Sahebic, G. Domairry, Numerical optimization of microchannel heat sink (MCHS) performance cooled by KKL based nanofluids in saturated porous medium, Journal of the Taiwan Institute of Chemical Engineers (2015) ⟨http://www.sciencedirect.com/science/article/pii/S1876107015001455⟩.

[25] J.Q. Zhu, K. Wang, C.Q. Nie, Computational research on film cooling under rotating frame by an anisotropic turbulence model, Propulsion and Power Research 2 (1) (2013) 20–29, URL ⟨http://www.sciencedirect.com/science/article/pii/S2212540X13000060⟩.

[26] M. Rahimi-Gorji, O. Pourmehran, M. Gorji-Bandpy, D.D. Ganji, An analytical investigation on unsteady motion of vertically falling spherical particles in non-newtonian fluid by collocation method, Ain Shams Engineering Journal, URL ⟨http://www.sciencedirect.com/science/article/pii/S2090447914001543⟩.

[27] O. Pourmehran, M. Rahimi-Gorji, M. Gorji-Bandpy, D.D. Ganji, Analytical investigation of squeezing unsteady nanofluid flow between parallel plates by LSM and CM, Alexandria Engineering Journal, URL ⟨http://www.sciencedirect.com/science/article/pii/S1110016814001069⟩.

[28] M. Hatami, D.D. Ganji, M. Gorji-Bandpy, Experimental and thermodynamical analyses of the diesel exhaust vortex generator heat exchanger for optimizing its operating condition, Applied Thermal Engineering 75 (22) (2015) 580–591, URL ⟨http://www.sciencedirect.com/science/article/pii/S1359431114008308⟩.

[29] B.J. hamrock, Fundamentals of Fluid Film Lubrication, Second ed., CRC Press, March 15, 2004.

[30] V.L. Streeter, Fluid Mechanics, Seventh ed., McGRA w-HILL, pp. 250-252.